# Design and manufacture of a basalt fibre reinforced polymer component for application in a highly efficiency electrical prototype

Diogo Tomé Fernandes Abreu Ribeira
diogo.ribeira@tecnico.ulisboa.pt

Instituto Superior Técnico, Universidade de Lisboa, Portugal

November 2019

**Abstract**

This work intends to evaluate the use of a mechanical component made from a composite material reinforced by basalt fibers as a replacement to another originally produced in aluminium, in this case, a support available in the steering system of an electric prototype. The starting point for this study was the analysis of the behaviour of the original support under the influence of a specific load. Once this data was obtained, computational simulations (Siemens NX 12) were performed, having the mechanical properties of the composite used been obtained through experimental tests. Finally, an optimization process was done in order to achieve the most suitable stacking sequence to use in the component to resist the loading. To conclude, a comparative study will be performed in order to assess the viability of using the alternative component.

**Keywords:** Basalt fibers, composite materials, finite element method, mechanical components, PSEM

## 1. Introduction

Over the last decades, there has been an exponential increase in the use of composite materials throughout the industry, with special focus on aeronautics and automotive. The use of these materials is largely due to the possibility of making more complex structures with less weight when compared to materials such as steel and aluminium. There are currently different types of fibres on the market, which can be split into two main groups: natural fibres, derivating from natural origin like plants, animals or soil, where the production process is also sustainable and, for instance, no chemical additives are used; and synthetic fibres, such as carbon and glass fibres, where the whole process of production requires several steps and the use of various chemicals in order to obtain a final product of high quality.

Having the various advantages of composite materials in mind, with a focus on the use of eco-friendly materials that contribute to a more sustainable future, which in turn enables the composite materials industry to decrease its environmental footprint, along with the possibility of applying a newly part to one of PSEM's (Projecto de Sustentabilidade Energética Móvel) project prototypes, made an interesting opportunity to test the use of composite materials with reinforcement materials (basalt fibres) uncommon among the project and even the industry.

PSEM's project is composed by students from Instituto Superior Técnico and aims at the development and subsequent construction of fully electric prototypes. The competition where the PSEM team is currently taking part is the GreenPower Education Trust - F24+ Championship. The rules of the competition [1] are made so that every team is forced to use the same electric motor and batteries, which are quite limited in terms of efficiency and energy density, thus the aerodynamics and weight represent important points to obtain a highly efficiency prototype. Figure 1 shows one of PSEM's prototype, GP 17 EVO.

Figure 1: GP17 EVO [2]

### 1.1. Fibre types

A comparative analysis between carbon and glass fibres, for being the most used in the industry, and basalt fibres, for being the ones considered in this work, will be performed.

The use of carbon fibres is now widespread across many industries due to the numerous advantages they provide. Although it is necessary to perform several steps that are very aggressive in terms of chemicals used up until the final product is obtained, which ends up being a slow process, once all issues related to the production are overcome, the fibres have many interesting properties such as high Young modulus when compared to commonly used metals, making them suitable for high demand applications; low thermal conductivity, high electrical conductivity and high resistance to chemically aggressive substances [3, 4]. For glass fibres the production process is simpler and very well known since these fibres have been used for many years now. This process has fewer steps than the ones needed for the carbon fibres, which means that it is a faster process. There are also some chemical agents involved but the main "ingredient" is silica sand, a very common material. Regarding the properties, these fibres present low thermal and electrical conductivity, making them a very good material for isolation purposes. Similar to what happens to carbon fibres, glass fibres also have a good chemical resistance, however, the Young modulus is lower than the previous ones [5, 6]. Finally, the basalt fibres (figure 2) are made from the volcanic rock basalt, which is the most common mineral on the Earth's crust. [7] The first idea for the basalt fibre production was patented in 1923, and since that period these fibres were classified as a material of military interest making them highly studied to discover new applications. Only many years later, in 1985, the creation of the first industrial facility for the production of basalt fibre made these fibres available for the general public.[8] Regarding the production method, this one is very simple, no additives are used just the rock, which is collected and transported to the factory where it is cleaned, smashed and melted to form "liquid basalt". After being liquefied, it is forced through an extrusion plate with hundreds of small holes, originating the basalt fibres. Concerning the properties of these fibres, one of the biggest advantages is that these fibres represent no harm to the human being, so they can be manipulated with minimal protection. Another advantage is the capability of resisting very high temperatures (around 600°C) without losing their properties [8, 9]. These fibres are also a good electric and acoustic isolators, and present a very good resistance to abrasion, being implemented in car parts like clutches and brake pads. Finally, it is verified that the Young modulus is slightly higher than the glass fibre's.

Figure 2: Basalt Fibres [Available in: https://basfiber.com/products]

In order to justify the statements made before and to better understand the differences between the three types of fibres, in table 1 some properties are presented.

Table 1: Characteristics of the three fibre types (Adapted from [10, 11, 12, 13, 14, 7, 8, 15, 16])

| | Carbon Fibre | Glass Fibre | Basalt Fibre |
|---|---|---|---|
| **Density [g/cm$^3$]** | 1.76 - 1.93 | 2.14 - 2.72 | 2.63 - 2.8 |
| **Young Modulus [GPa]** | 230 - 588 | 51.7 - 86 | 79.3 - 110 |
| **Ultimate Stress [MPa]** | 3500 - 7000 | 2415 - 4890 | 2800 - 4840 |
| **Elogation at break [%]** | 1 - 2.2 | 4.4 - 5.7 | 3.1 - 6 |
| **Thermal Conductivity [W/mK]** | 3 - 55 | 1 - 1.05 | 0.031 - 0.038 |

### 1.2. Insert

As opposed to metallic components, which are bonded using bolted and welded connections, the attachment of composite material parts present some difficuties due to the inability of performing those connections. A widely used alternative is the placement of a small portion of a metal material, called insert, within the composite considered, thus facilitating bolted connections between different components.

## 2. Determination of geometry and materials properties

### 2.1. Original Component

In order to assess the influence of using basalt fibres on a prototype's component, it was chosen a part that was already in use and made from metal (7075 – T6 aluminium). After the process of

choosing the component that brought together the best conditions for this test, it was decided to use the wheel hub carrier support. Its location, on the prototype, is illustrated in figure 3.

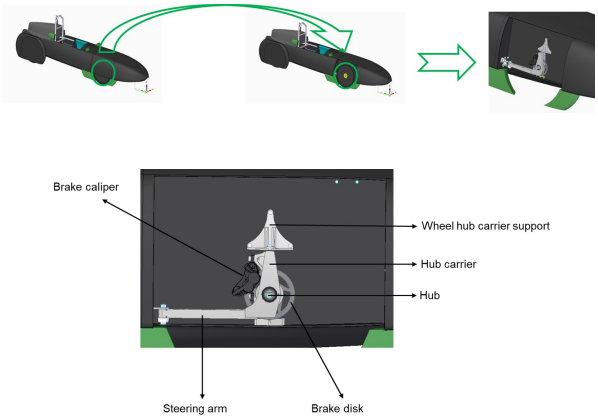


Figure 3: Wheel hub carrier support location

This component is part of the steering system of the prototype and its main role is attaching the system to the structure, using three M5 bolts, while allowing wheel rotation so the prototype can make all the turns in the race circuit. The rotation movement is achieved by using a radial spherical plain bearing placed on the central bearing housing in the component's bottom part. The connection between the support and the remaining part of the steering system is also made by an M5 bolt on the central hole. In Figure 4, an exploded view of the parts used in the support assembly is displayed.

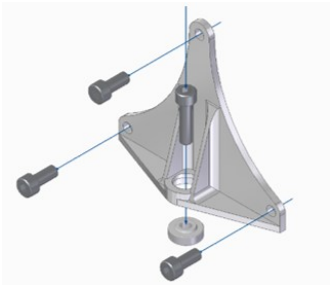

Figure 4: Exploded view of the wheel hub carrier support assembly (bolts and radial spherical plain bearing)

2.2. Determining Loads

Using the CAD (Computer Aided Design) program (Solid Edge ST10) where the prototype was designed, it was possible to assess its weight and make an estimate of the center of mass of the prototype + pilot system, and also the position of the contact point between the support and the remaining steering system. This is displayed in figure 5.

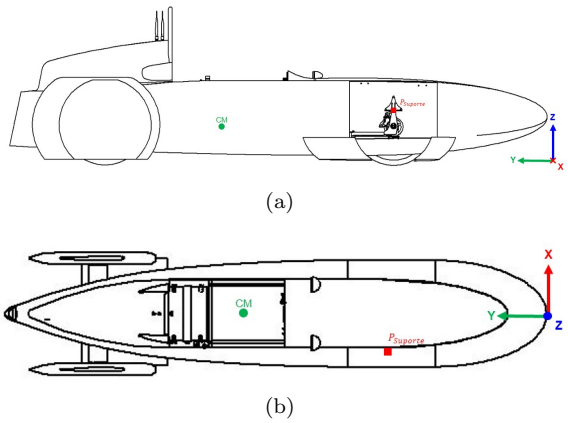


Figure 5: GP17 EVO prototype drawing view with center of mass and contact point (a) Lateral view (b) Top view

All the information obtained from the CAD program was later confirmed by experimental data, weighing the prototype using 4 scales. Using simple static analysis, and considering the prototype coordinate system, it was possible to calculate the loads that were applied to the support. In figure 6 it is shown where the loads are applied to the support, meaning the contact point between the support and the remaining steering system.

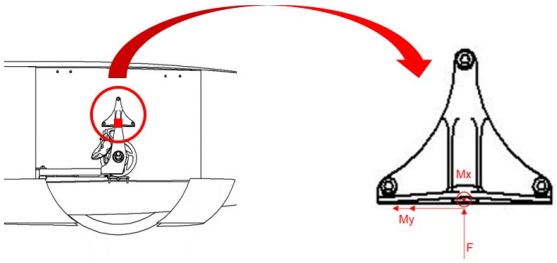


Figure 6: Loads applied on the wheel hub carrier support

In order to avoid problems during the component's use, it was implemented a safety coefficient using the Pugsley method [17], consisting on using several empirical data such as the material quality or the economic impact if the failure were to occur, which generates an oversize loading. The factor considered for this case was 2.73, resulting on the final loads that would be taken into account for future analysis. The loads are presented in table 2 and they are applied as shown in figure 6.

Table 2: Values of the applied loads

| **F [N]** | **$M_x$ [Nm]** | **$M_y$ [Nm]** | **$M_z$ [Nm]** |
|---|---|---|---|
| 692.30 | 575.58 | 104.30 | 0 |

2.3. Looking for a new solution

For the implementation of a new support made from a composite reinforced by basalt fibres to be made possible, it was necessary to design a new component that allows the manufacturing to be done with that specific material. So, the first step was performing a finite element method (FEM) analysis, using a commercial software (Siemens NX 12), on the original component made from aluminium. The mechanical properties [18] considered for this analysis are shown in table 3.

Table 3: Aluminium 7075-T6 mechanical properties

| | |
|---|---|
| **Density [Kg/m$^3$]** | 2810 |
| **Young Modulus [GPa]** | 71.7 |
| **Poisson Coefficient** | 0.33 |
| **Shear Modulus [GPa]** | 26.9 |

Once the behaviour of the part under the influence of the loads described before was examined, it was possible to analyse what the characteristics that would need to be changed or maintained in the new part are. The second step when starting the new part's design, is to maintain the position of all fixing points responsible for connecting it to the prototype structure and also the point used to attach it to the remaining steering system components unchanged so when the support was used in the prototype it would fit perfectly. Taking into consideration all the information acquired regarding the geometric constraints and the original component's behaviour, several new possibilities for a new component were examined. The FEM analyses performed, using a generic stacking sequence, were preliminary and were used to assess the behaviour of the many components' geometries designed, until a final one was chosen. The mechanical properties for the basalt fiber composite considered for these computational simulations were computed from the properties of the chosen matrix (epoxy resin) and reinforcement (basalt fibers) and introduced in the FEM program, allowing it to perform the calculations to obtain the lamina (BFRP - Basalt Fiber Reinforced Polymer) properties present in the table 4.

Table 4: BFRP generic mechanical properties

| | |
|---|---|
| **Density [Kg/m$^3$]** | 2001 |
| **$E_1$ [GPa]** | 28.41 |
| **$E_2$ [GPa]** | 28.41 |
| **$G_{12}$ [GPa]** | 2.80 |
| **$G_{13}$ [GPa]** | 2.72 |
| **$G_{23}$ [GPa]** | 2.21 |
| **Poisson Coefficient** | 0.08 |

All the geometries studied, shown in figure 7, had some problems and they were rejected for various reasons until a final geometry for the support proved to have good characteristics to be a possible replacement for the original component.

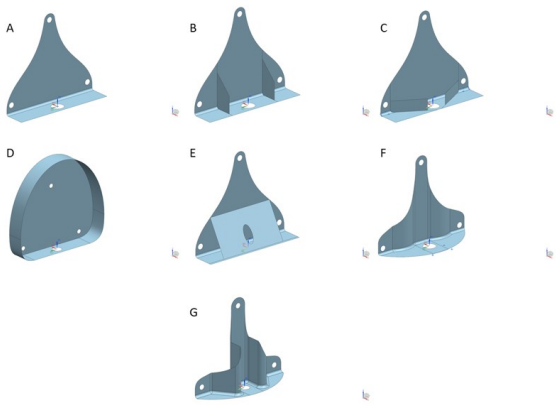


Figure 7: Different geometries designed

The starting point was geometry A, for it was a very simple one and so the new material behaviour and the adjustments needed could be easily assessed. But as expected, the deformation observed was higher when compared with the original support. The geometries B and C tried to minimize that problem with the use of two vertical ribs, which helped with the problem but also introduced a new one, with the possibility of the reinforcements to be poorly glued to the structure, originating many problems resulting in the component's failure. To try to solve this problem, geometry D was created but quickly it was concluded that its weight was very high, ending with its rejection. So, geometry E was created but after some research, the idea of using glued reinforcement was abandoned. So a way to have reinforcements without having to glue them was necessary, thus geometry F appeared, but after further analyses, the deformation observed was still high. So geometry G was created, showing a decrease in mass and improved characteristics regarding the deformation and stresses when compared to the original one.

2.4. Determination of composite properties

The properties of basalt fibres vary according to the location from which the raw material is collected, so to make credible predictions of the behaviour of fibre reinforced structures it is important to characterize the composite that will be utilized. The basalt fibres were supplied by Basaltex and have the reference BAS 220.1270P, and the matrix element was an epoxy resin produced by Sicomin - SR1500 to mix with SD 2505 hardener.

In order to determine the mechanical properties for this composite two test methods developed by ASTM (American Society for Testing and Materials) were chosen. The chosen methods were the ASTM D 3039 and ASTM D 3518; both can be used in the mechanical characterization of composite materials reinforced by fibres. The experimental procedure suggested by the two tests method was followed starting by the manufacturing of two plates, with the appropriate stacking sequence, after that the plates were cut to the specimen's required dimensions and instrumented. Once this process was finalized, the specimens were ready to be tested. Five specimens were tested, and the mechanical properties obtained are as shown in table 5.

Table 5: BFRP final mechanical properties

| | |
|---|---|
| **Density [Kg/m$^3$]** | 1750 |
| **$E_1$ [GPa]** | 18.62 |
| **$E_2$ [GPa]** | 18.62 |
| **$G_{12}$=$G_{13}$=$G_{23}$ [GPa]** | 2.90 |
| **Poisson Coeficient** | 0.104 |

## 3. Optimization Process

Once the final properties for the composite that would be used in the alternative component had been obtained, an optimization process of the laminate regarding the number of layers required and its orientation was performed. This would not only allow obtaining the small mass possible for the part but also making the component tougher to the applied loads by improving the ply stacking in the laminate considered.

A computational program was developed deliberately for this task using the *MATLAB® R2018b* software. The program was developed in order to obtain the best stacking sequence (number of layers and orientation) for a certain defined geometry, taking into account the maximum deformation found in it. This program would also be responsible for the interaction with the finite element solver, associated with the commercial program called *Nastran*. The optimization program works together with the computational FEM program to evaluate every possible stacking sequence. The first step executed by the Matlab program is to read the problem variables from a text file (**.dat*) generated by the FEM program. The file is read and the location related to the stacking sequence is found, and then changed. The file is saved and the finite element solver is initialized. Once the simulation is over, the MatLab program reads the output file generated by Siemens NX 12, **.f06*, and locates the required data - the mass and the maximum deformation verified in the structure. Figure 8 shows an outline of the steps performed by the optimization program.

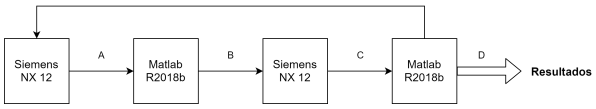


Figure 8: Optimization process schematic

A – *.dat File B – Stack change and *Nastran* execution
C – *.f06 File D – Ccompilation and presentation of results

The program is terminated when all the possible stacking sequences have been analysed. To finalize, the optimization program orders the stackings, from the one with less deformation and smaller mass to the one on the opposite end. In order to simplify the optimization process, avoid long processing times and also taking into account the applicability of the component, it was initially defined that the component laminate would consist of 10, 12, 14 or 16 layers of the composite considered, and it would also be symmetric to avoid some problems, like bending. Another simplification that would be used was to only consider layer orientations at 0º and 45º since the fibre used is woven and, therefore, the fibres end up being oriented in the same way with each 90º rotation, so considering ply orientations of 90º or -45º would be redundant.

Analysing the results obtained, and comparing the deformations verified with the masses obtained for each stacking sequence analysed, it is possible to conclude that the stacking that presents the most advantages is the stacking with 10 layers, where the fibres orientation are $[0/0/0/45/0]_s$.

## 4. Obtaining the component and experimental testing

### 4.1. Final simulation

Once the best stacking sequence regarding the parameters pre-defined had been choosen, a final finite element analysis was performed in order to obtain all the relevant data (stresses, strain, deformation) for the alternative component.

### 4.2. Mould

Having all the required analyses been finished, the component needed to be manufactured. In this case, CNC machined mould, from a solid block of polyurethane, named SikaBlock M 700 (figure 9) was used. This material was chosen because of its good compatibility to produce composite materials, ease of machining, and ability to produce a good surface finish.

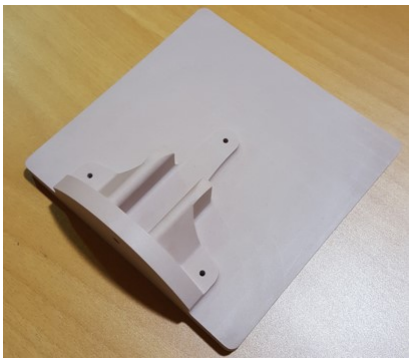

Figure 9: Mould for the wheel hub carrier support

### 4.3. Component Manufacturing

With the mould finalized it was necessary to follow a few steps to obtain the final component. The manufacturing process was done in Escola Superior de Tecnologia - Instituto Politécnico de Setúbal. The steps were as follows:

- Mould preparation. The firt stage was sealing the mould since its surface is very porous, after that a demoulding agent was apllied so the final part could easily be removed from the mould.

- Basalt fibre cutting. The required basalt fibre sections were cut using paint tape around its perimeter in order to avoid fibre distortion. Ten fibre layers were cut following the orientations obtained through the optimization program.

- Matrix preparation. The resin and the hardener were mixed according to the product datasheet.

- Component manufacture. Every layer of basalt fibre was impregnated individually and then placed on the mould. The manufactured process was the vacuum assisted hand lay-up. The mould was hold under vacuum for a period of 24 hours to assure a complete resin cure.

- New component. Once the 24 hours period is over the component is ready to be demoulded.

Upon inspection of the component produced, some defects were found, especially in areas where a small curvature is observed, it was noticed that the fibre was not correctly positioned, leading to an abnormal accumulation of resin in those areas, as illustrated in figure 10.

Figure 10: Component's defects

Another defect found was the presence of portions of the release film that got stuck on the manufacrure part and could not be removed, which may result in a weakening of the bond between the fibre layers, resulting in structural problems in the component.

Thereafter, an attempt to correct the problems exposed led to a second try. The procedure followed was similar, the main difference verified being in the fibre cutting step, which was performed having the sections cut to an approximate shape of the component, instead of just quadrangular fibre sections as before. Another difference was the way plies were placed on the mould, this time the procedure followed was placing them in two groups of 5 layers each. The composite cure process was done two times, meaning the first 5 layers and the insert and after the remaining layers (figure 11).

(a) (b) (c) (d)

Figure 11: Component's manufacture: (a) Basalt fibre cutting procedure (second component) (b) Plies and insert placement on the mould (c) Vaccuum assisted hand lay up process (d) Final component

Once the second component executed was

demoulded, it was possible to observe that the defects were eliminated. So, in order to obtain a component with a geometry equal to the idealized one, it was necessary to carry out a finishing process to eliminate all fibre excess resulting from the production process, drilling all the necessary holes and machining the housing for the plain bearing (figure 12).

Figure 12: Bearing housing machining

The finishing process was applied to both components manufactured.

4.4. Experimental tests

To validate all the process it was decided to perform an experimental test to both parts. To make experimental data gathering possible three strain gauges were placed on the second component on the grounds that it was the only one which presented no defects.

To make carrying out the experimental test possible, an experimental setup was designed and machined (figure 13), so the test conditions can reproduce the ones present when the component is being used in the prototype, meaning the camber angle. The experimental tests were performed, in an universal testing machine - Instron 5566, and on both components even though the first one had some defects. The procedure for testing the first component was applying a continuous force until the component's failure, whereas for the second, in order to record the values measured by the strain gauges, the test was performed manually and by steps, starting at 0 N and making increases of 500 N until the component fails.

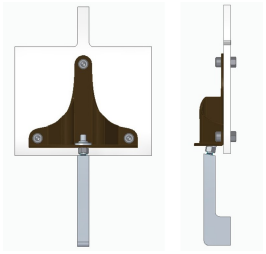

(a)

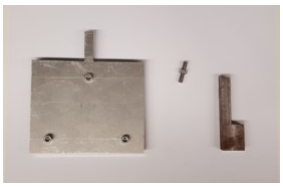

(b)

Figure 13: Experimental setup: (a) Experimental setup in CAD (b) Experimental setup machined parts

## 5. Results and discussion

In order to assess how the new solution had advantages or disadvantages over the existing component, a comparison of several parameters (mass, strain, stress and deformation) of interest was made so that a conclusion can be produced, and the applicability of the new component can be evaluated.

In order to compare the values measured by the strain gauges placed on the component, there were "zones" created on the finite elements component corresponding to the strain size and location (figure 14). Then the strain measured by the elements inside that area was recorded and compared to the values obtained during the experimental testing.

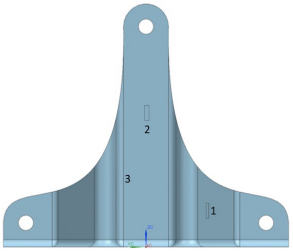


(a)

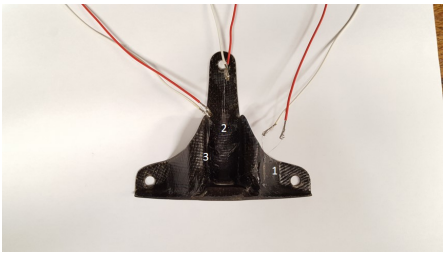


(b)

Figure 14: Strain gauges representation (a) On the CAD component (b) On the manufactured component

The values recorded on the component MEF analysis are presented in the table 6.

Table 6: Strain values obtained from the finite element simulations

| | **Strain - Zone 1** [$\mu\epsilon$] | **Strain - Zone 2** [$\mu\epsilon$] | **Strain - Zone 3** [$\mu\epsilon$] |
|---|---|---|---|
| 0 N | 0 | 0 | 0 |
| 500 N | 70.72 | -675.99 | -137.27 |
| 1000 N | 141.43 | -1351.99 | -274.55 |
| 1500 N | 212.15 | -2027.98 | -411.82 |
| 2000 N | 282.85 | -2703.97 | -549.09 |

The values recorded during the experimental test are displayed and in table 7.

Table 7: Strain values obtained from experimental testing

| | **Strain Gauge 1** [$\mu\epsilon$] | **Strain Gauge 2** [$\mu\epsilon$] | **Strain Gauge 3** [$\mu\epsilon$] |
|---|---|---|---|
| 0 N | 0 | 0 | 0 |
| 500 N | 67 | -876 | 0 |
| 1000 N | 102 | -1390 | -77 |
| 1500 N | 150 | -2093 | -190 |
| 2000 N | 220 | -3055 | -312 |

The first conclusion to be drawn is that the values are consistent between the simulations and the experimental tests. From the observation of the data of the first and second strain gauges, it is concluded that the values obtained in the tests are close to those obtained in the simulations. Regarding the third strain gauge, it can be observed that the data obtained are quite different, something that may be justified by a misplacement of the strain gauge, which may have been misaligned with the fibres orientation or for any damage it may have suffered when handling or assembling the component in the testing machine. Another possibility that may help to explain the variation between the simulated and experimental values is that during the manufacturing process some of the fibre layers might have had some distortion and had not been correctly positioned in the mould, since in the simulations the program considers the "perfect case" where the fibres are perfectly aligned and with no distortion. Table 8 shows the values of the experimental errors that support the previous statements.

Table 8: Experimental Errors

| | **Error 1** [%] | **Error 2** [%] | **Error 3** [%] |
|---|---|---|---|
| 0 N | 0 | 0 | 0 |
| 500 N | 5.25 | 29.58 | 100 |
| 1000 N | 27.88 | 2.81 | 71.95 |
| 1500 N | 29.29 | 3.21 | 53.86 |
| 2000 N | 22.22 | 12.98 | 43.18 |

Another point that can be compared is the force required to break the component: the first one to test reached 3388 N whereas the second only reached 2365 N. This is quite a difference, especially when compared with the value estimated by the computational simulations which were 4773 N. The difference verified between the two components can be justified by the manufacturing process for the two components, doing the second one in two steps may have introduced some defects in it, like a decreased in the fibre adhesion or any other type of contamination during the second cure process. Yet, it was possible to observe that the component's failure happened in the same area (figure 15).

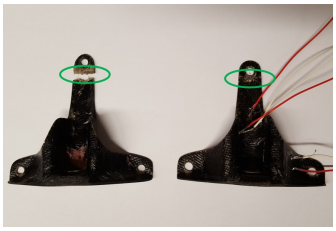

Figure 15: Components's failure

To try explaining this event the computational simulation for the last applied force that was possible to collect data from the strain was checked (figure 16)

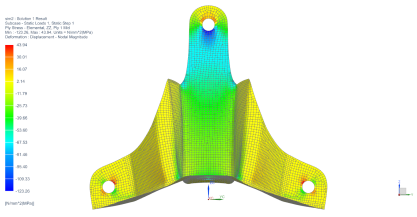

Figure 16: Stress $\sigma_{zz}$ observed in the component for a load of 2000 N

By analysing the stress data it was observed that there is a stress concentration near the upper hole, with values of approximately 120 MPa (compression), when the average value verified in

the component is approximately 20 MPa. Since the failure of both components occurs in approximately the same zone, it can be claimed that the cause of the failure is the stress concentration which made that area susceptible to having problems during the component use.

To conclude, figure 17 shows the original and alternative components, allowing for a better perspective of the differences regarding the geometry.

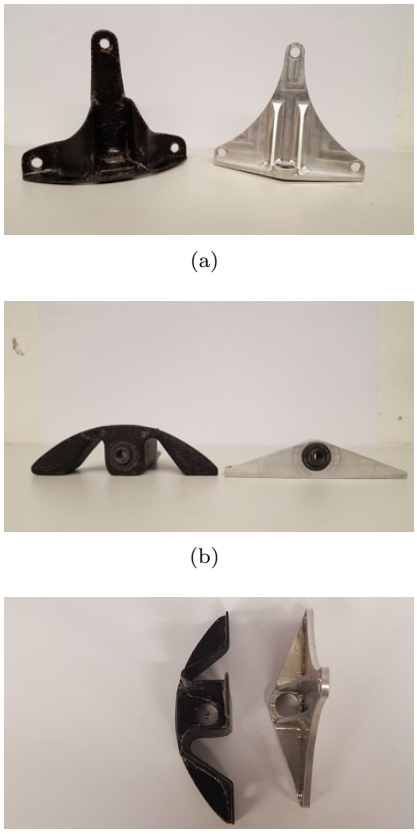

(a) (b) (c)

Figure 17: Alternative component vs Original component: (a) Frontal view (b) Bottom view (c) Top view

Once the differences in the shape of the components were verified, a comparison of some relevant parameters was made in order to verify the consequences of the changes made. Thus, table 9 presents some of the considered parameters, taking into account the previously calculated load.

Table 9: Comparison between the original component (O C) and the alternative component (A C)

| | Mass [g] | Maximum Deformation [mm] | Maximum Stress [MPa] |
|---|---|---|---|
| **O C** | 40 | 0.02 | 66.73 |
| **A C** | 22 | 0.09 | 45.85 |
| **Variation** [%] | -45 | 350 | -31.29 |

Considering the obtained values, it is verified that the mass value of the alternative component is quite inferior, resulting in a 45% reduction in the total mass of these components in the prototype. Regarding the stresses in the components, lower values are also verified in the component produced by composite material, which may lead to a longer life of said component. The deformation presented corresponds to the maximum value verified in the vertical direction (z), which is higher in the alternative component, since the capacity of fibre reinforced composites to resist loads is smaller when compared with aluminium since it has a higher Young modulus. However, the values considered are quite small and the discrepancy verified in them does not produce negative consequences in the whole steering system. The ideal situation would be to reduce deformation, however, the advantages added by the new component largely compensate for the disadvantages that may have been added.

## 6. Conclusions

Analysing the work developed, it is possible to state that the hypothesis of the use of basalt fiber reinforced composites in parts as replacement of others made in metal (aluminum 7075 - T6) is a viable alternative. Due to all the variables present which are difficult to control, such as track irregularities, accidental fall of the prototype during handling or imperfections during the manufacturing process, the entire study took into account an oversizing of the applied load, so the obtained result is conservative.

During the specimens experimental testing some problems with the strain gauges were verified resulting in obtaining measurements from only 3 specimens rather than from the five that were tested. Regarding the optimization process, this was a slow process taking around three hours in order to analyse all the stacking possibilities considered. Concerning the data gathered from the strain gauges mounted on the tested component, the experimental errors verified are inferior to 30% which corroborates the

computational simulations performed and also the manufacturing process followed.

### 6.1. Future Work

As a way of trying to give out a more detailed explanation of some situations verified during this work, and also in the perspective of continuing to present developments on the subject of basalt fiber reinforced composite materials, the following ideas are presented:

- Carrying out a further optimization process taking into account the possibility of considering different stacks in different areas of the component geometry in an attempt to further reduce the mass and also increase the stiffness.
- Carry out a comprehensive analysis with the execution of specimens and perform experimental tests in order to verify if there is influence of the procedure followed during the composite manufacture, meaning, if there is any significant change in the mechanical properties when a composite with 10 layers is either manufactured in a single step or two steps.
- As the team seeks to participate in more and more races, it would be interesting to perform a fatigue analysis in order to obtain an estimate of the number of cycles to which the component can be subjected.
- Considering the recyclability of basalt fibers, study the compatibility and mechanical properties when combined with bio-resin in order to obtain a composite with less environmental impact.

## References


[1] Greenpower tecnhnical regulations. https://www.greenpower.co.uk/sites/default/files/uploads/Technical%20and%20Sporting%20Regulations%202019%20V1.2.pdf. (Accessed in December 2018).

[2] Psem website. http://psem.ist.utl.pt/en_pt/about_us.html/. (Accessed in December 2018).

[3] How is carbon fiber made? http://zoltek.com/carbon-fiber/how-is-carbon-fiber-made/. (Accessed in June 2019).

[4] The making of carbon fiber. https://www.compositesworld.com/articles/the-making-of-carbon-fiber. (Accessed in 2019).

[5] The making of glass fiber. https://www.compositesworld.com/articles/the-making-of-glass-fiber. (Accessed in June 2019).

[6] How products are made - fiber glass. http://www.madehow.com/Volume-2/Fiberglass.html. (Accessed in June 2019).

[7] Vivek Dhand, Garima Mittal, Kyong Yop Rhee, Soo-Jin Park, and David Hui. A short review on basalt fiber reinforced polymer composites. *Composites Part B Engineering*, 12 2014.

[8] Anthony R Bunsell. *Handbook of properties of textile and technical fibres*. Woodhead Publishing, 2018.

[9] V Fiore, T Scalici, G Di Bella, and A Valenza. A review on basalt fibre and its composites. *Composites Part B: Engineering*, 74:74–94, 2015.

[10] Ever J Barbero. *Introduction to composite materials design*. CRC press, 2017.

[11] Carbon fiber - mechanical properties. http://www.torayca.com/en/lineup/product/pro_001_01.html. (Accessed in June 2019.

[12] Carbon fiber - mechanical properties. https://www.hexcel.com/Resources/DataSheets/Carbon-Fiber. (Accessed in June 2019).

[13] Glass fiber - properties. https://www.vetrotextextiles.com/technologies/fiberglass-manufacturing/fiberglass-properties. (Accessed in June 2019).

[14] Sathishkumar T P, S Satheeshkumar, and Naveen J. Glass fiber-reinforced polymer composites - a review. *Journal of Reinforced Plastics and Composites*, 33:1258–1275, 06 2014.

[15] Kunal Singha. A short review on basalt fiber. *International Journal of Textile Science*, 1(4):19–28, 2012.

[16] The basalt fiber history. http://www.basaltft.com/hist.htm. (Accessed in July 2019).

[17] Steven R Schmid, Bernard J Hamrock, and Bo O Jacobson. *Fundamentals of machine elements: SI version*. CRC Press, 2014.

[18] Aluminium supplier. http://www.kms.com.pt/index.html.